Simulation and flight test of a temperature sensing stabilisation system

P. Herrmann and C. Bil
Sir Lawrence Wackett Centre for Aerospace Design Technology
School of Aerospace, Mechanical and Manufacturing Engineering
RMIT University
Melbourne, Australia

ABSTRACT

Thermopile sensors detect electromagnetic radiation as a function of the object's temperature. Because there is a temperature difference between the cold ground and the warm sky, these sensors could be used to detect the horizon and thus be used as a reference to stabilise a small aircraft, such as an unmanned aerial vehicle (UAV) in visual meteorological conditions (VMC). To verify this hypothesis, a system has been developed providing horizon detection using thermopile sensors to stabilise an R/C model aircraft. The aircraft has gone through a number of flight trials using remote control to enable and disable the stabilisation system. During the flight trials the aircraft was set at various attitudes when the system was enabled. The stabilisation system was able to assume wing level under various bank angles and weather conditions with minimum overshoot and oscillation.

Although the system shows good performance during flight trials, most of the original design was done using trial and error. A design tool was needed to implement further improvements to the system and to efficiently implement it on other aircraft. This required a good understanding of the physical behaviour of the system and the interaction between the sensors, aircraft and the environment. A mathematical model of the overall system was developed using the MATLAB/Simulink environment to simulate the behaviour of the system under various conditions. The simulation results were then compared with actual flight experiments. This paper describes the modelling techniques used for the different system components and the results of the simulation compared to actual flight trials.

1.0 INTRODUCTION

1.1 Atmospheric temperature sensing – background

All matter emits electromagnetic radiation as a function of its temperature. In this application thermopile sensors are used to distinguish the relatively cold sky from the warm ground. It is essential that the abient visibility is sufficient such that the sensors are able to reliably detect this differential. In cases with very low visibility, such as inside cloud, the thermopiles would be measuring the differential across a very small column of air. This is not expected to provide a reliable signal, despite the sensors being capable of detecting very small temperature differentials; the main limitation in this case would be local turbulence and mixing of the air, causing local temperature inversions and the like.

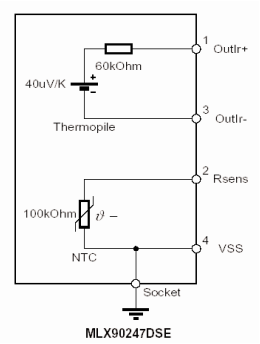
A sensing system incorporating thermopiles was designed, built and tested on a model aircraft to detect the horizon and use it as a reference to stabilise the aircraft. This technique offers a low-cost solution for the stability and control on model aircraft and UAVs operating in VMC.

Thermopiles are essentially a micro array of dissimilar metal junctions with hundreds of very thin, thermally isolated 'hot junctions' exposed to incoming radiation and the 'cold junctions' thermally bonded to the sensor case. A silicon IR filter restricts the incoming radiation to a narrow band of the IR spectrum (8-14μm). This band is selected for sensitivity to blackbody radiation from objects with a temperature in the range between –75°C to 75°C. Conveniently, the Earth's atmosphere provides good transmission in this narrow range. See Taylor[8] for a more complete description.

Paper No. 2904. Manuscript received 22 July 2004, revised version received 16 March 2005, accepted 6 April 2005.
This paper was first presented at the 19th Bristol International UAV Systems Conferences.

https://doi.org/10.1017/S0001924000000671 Published online by Cambridge University Press

Manufacturer / Model No.	**Melexis 90247 DSE**
Sensitivity (μV/degK)	**29 / 40 / 55**
min/typ/max	
Package	**TO–39**



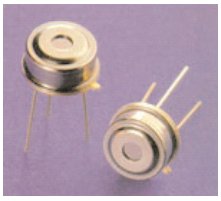


Figure 1. Melexis 90247 thermopile sensor specifications.

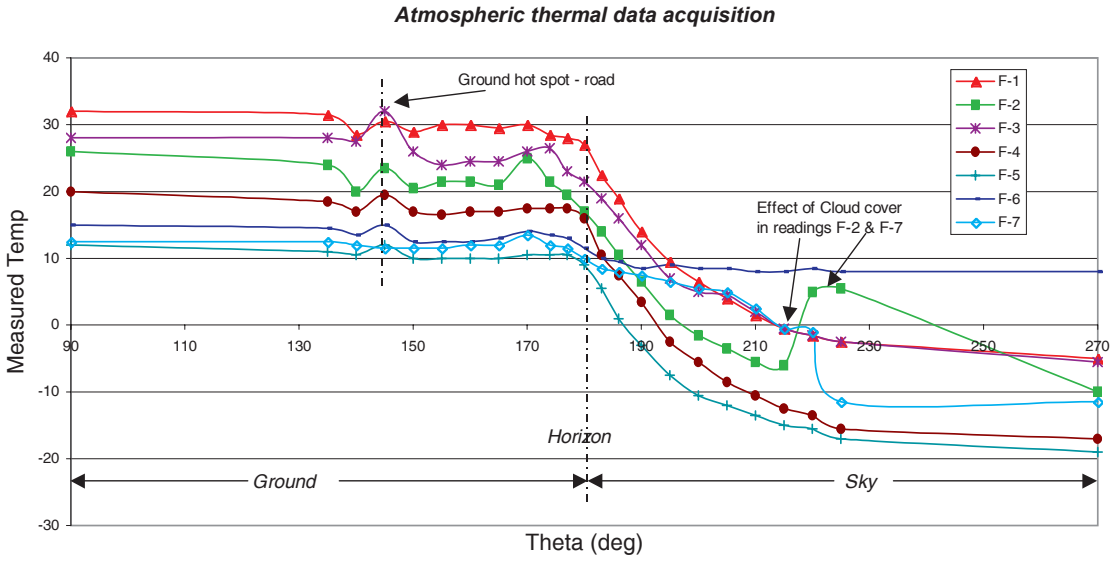


Figure 2. Plots of temperature *vs* azimuthal angle for a series of recordings under differing weather conditions.

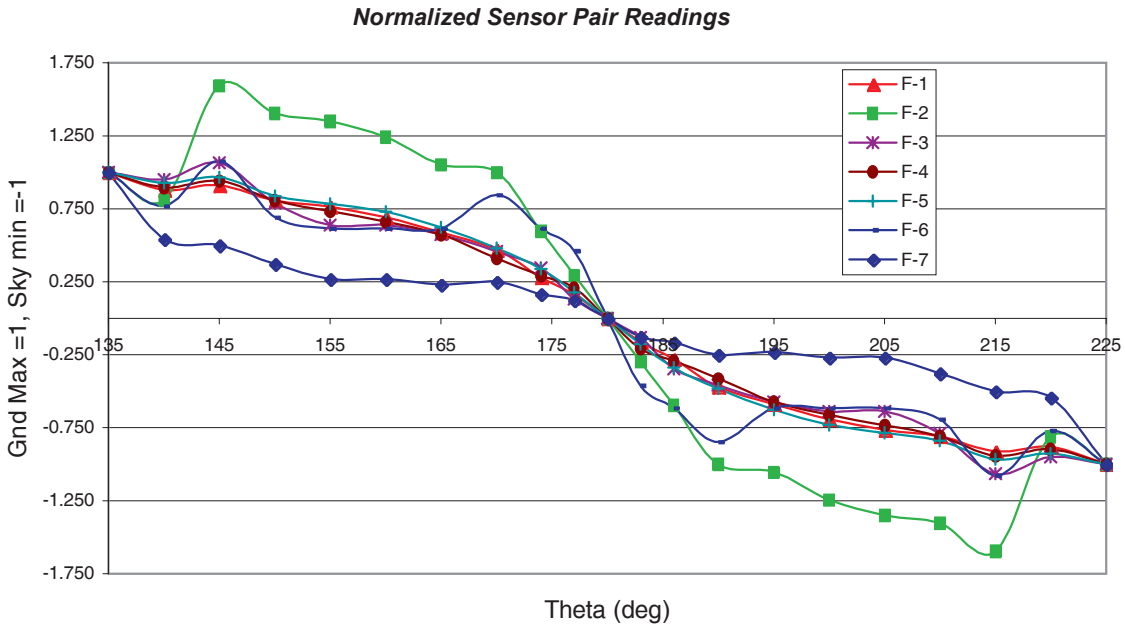


Figure 3. Normalised sensor pair readings derived from Fig. 2 data.

https://doi.org/10.1017/S0001924000000671 Published online by Cambridge University Press

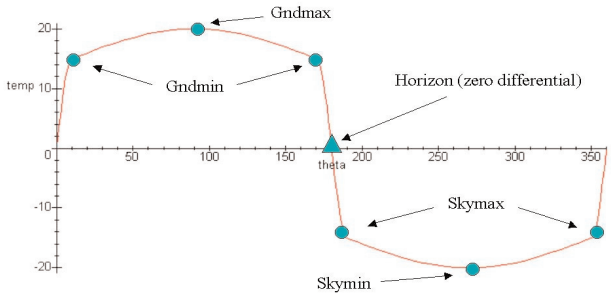


Figure 4. Atmospheric temperature model representing one axis (pitch or roll). Note that 180° and 360° represent the horizon in each direction.

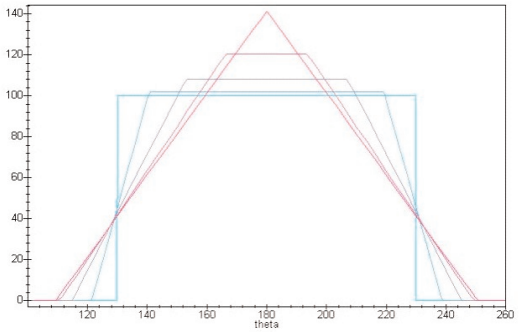


Figure 5. Influence functions for a range of sensor rotation angles (φ).

1.2 Thermopile sensor specifications

Figure 1 shows the technical details of the thermopiles used, including a functional diagram of the thermopile sensor. Note that NTC temperature sensor is not used, as the absolute temperature is not required, only the differential of the pair of sensors, which are in series, arranged 'back to back'. This approach assumes that the case temperature of both sensors is the same.

2.0 ATMOSPHERIC THERMAL MODELLING

In order to model and evaluate the performance of this guidance system, we first need to gain some insight into the thermal signal radiated from the environment around the aircraft. As thermopile sensors are commonly employed in non-contact thermometers, the use of such a device provided a simple method of obtaining temperature data in a variety of atmospheric conditions. The unit used (Raytek MT-2 Minitemp) had a field of view of 20º, substantially narrower than the naked Melexis sensors being used in the autopilot system; these are believed to provide a square field of view (FOV) of 100º. Note that these sensors are less sensitive than those in the Raytek to fine detail because any thermal irregularity will occupy a smaller portion of the FOV.

The readings shown in Fig. 2 are for a single sensor producing an absolute temperature value. The ground temperature is relatively warm in comparison to the cold sky, which may read as low as –30ºC in clear (no cloud or precipitation) conditions. This trend is the fundamental concept that is to be exploited to provide attitude control. The autopilot sensors comprise of a differential pair of sensors about two axes (pitch and roll). As no suitable hardware was available at the time of testing, the sensor pair was simulated by assuming that the atmospheric temperature distribution is symmetric about the vertical plane. By observing the above assumption, the data was normalised with respect to the minimum/maximum (sky/ground) temperatures, and the results are shown in Fig. 3.

Of the sample data shown, four plots behave in an expected and repeatable manner. The region of greatest change occurs near the horizon providing the highest sensitivity. The remaining three readings (F-2, F-6 and F-7) show sensor response under different adverse conditions.

F-2 – is typical of the effect of high, patchy cloud cover. The performance within ±30º of the horizon is generally good, but the influence of the warm clouds (5ºC Approx) present above 40º from the horizon cause the differential measurement to be lower than under clear conditions. Given that the control gain is derived from the maximum sky-to-ground temperature differential, such conditions generate an artificially high gain. This is visible on the normalised plot as regions where the value exceeds the bounds of 1 and –1.

F-7 – is also the result of patchy cloud cover, this time extending from the horizon (180º) to 220º. Since the gain is based on the clear sky reading, it will be lower than optimal at angles where clouds are visible.

F-6 – this reading shows the normalised response under overcast low cloud cover. In this case the maximum differential temperature is reduced to only 7ºC. (4ºC Was the smallest observed during testing, 20-30ºC is typical in clear conditions.) 'Noise' is apparent here as small variations in sky and surface temperature have a relatively large influence given the high gain associated with this small maximum differential temperature.

Analysis of these atmospheric thermal measurements highlights several challenges & potential pitfalls of such a system. Degraded performance would be expected in cases of very low maximum temperature differential (MTD). Two factors are important here, the actual measurement resolution of the system and the impact of hot or cold spots appearing within the sensor FOV. The prototype system has flown successfully in hazy conditions where the MTD was only 3ºC. Safe operation inside dense cloud is not expected due to the MTD being virtually zero in these instances. However, operation between bands of cloud is expected to be possible due to the adiabatic lapse rate causing a measurable temperature differential between cloud layers. Note that the averaging effect of having a wider FOV will allow the actual system to cope better with irregular cloud coverage and ground based 'hot spots' than these tests results indicate. This integration or averaging effect of the source field within the FOV is addressed in the simulation.

In order to model the controller behaviour in varying atmospheric conditions, a generic atmosphere temperature model was created, simulating the sensor pair response. The approach was to build a model representing the temperature around 360 degrees of rotation (roll or pitch). Based on the previously examined test data and taking into account the field of view that the Raytek (see previous section) unit had, the following model was constructed in Maple[5]. It consists of three discontinuous heaviside functions, two sinusoids representing 160º of ground and sky respectively and a cubic spline fitted between the remaining 20º at each horizon, joining the two sinusoids together (Fig. 4). The original approach was that four temperatures could be specified (Ground max and min, Sky max and min) as indicated below. Since the temperature measurement is differential this model only requires two independent inputs. The approach was then to perform definite integration over a range of 100º, representing the viewing angle of the thermopiles. The mid point of this integration range represents the orientation of the sensor and the integral divided by the viewing angle is the measured temperature. This process was conducted in a loop to calculate the response of the sensor pair around a complete revolution. The output was left in terms of the defining temperatures (Ground max and min) and exported as a matrix, forming a lookup table within the dynamic Simulink model[6,7]. This approach added negligible computation time to the dynamic model, while allowing realistic sensor performance to be simulated.

https://doi.org/10.1017/S0001924000000671 Published online by Cambridge University Press

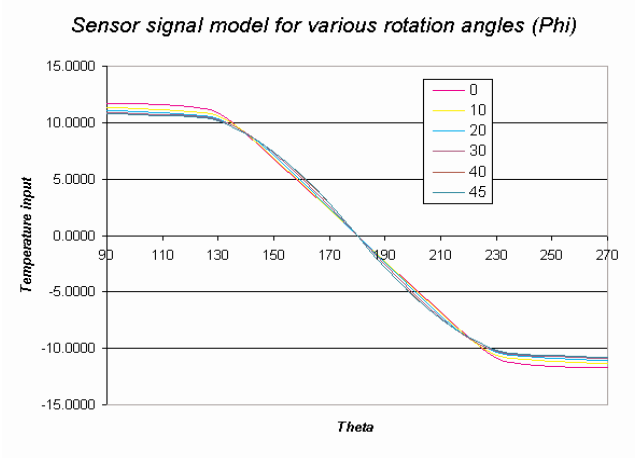


Figure 6. Sensor response *vs* rotation angles.

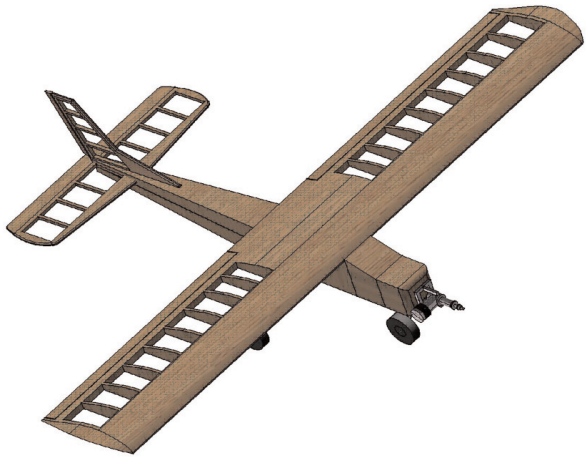


Figure 7: Trainer model used in flight tests (wingspan = 1·6m).

As the field of view of the thermopile sensing elements is square (100º in each direction) an 'influence function' was incorporated in the above integration process. This allows for the orientation of the sensing elements with respect to the horizon. It is assumed that each sensor is aligned with its differential pair. A series of these influence functions are shown in Fig. 5, for a range of sensor rotation angles from 0º to 45º. For example, if the pitch angle of the aircraft is zero, then the roll influence function is constant throughout the sensors' field of view, represented by the cyan square in Fig. 5 ($\varphi = 0º$). If the aircraft were now to pitch 45º nose up, the sensitivity of the roll sensor would now be altered such that the pink triangle represents its effective field of view ($\varphi = 45º$).

This method is strictly only valid for small angles, since at larger angles one axis will affect the sensitivity of the other.

In an extreme case, for example nose pitch up 90º, the sensitivity of the roll axis is now zero since the roll sensor pair will 'see' the horizon regardless of their position (ϕ).

This is only a limitation of the current model and does not imply that the real controller cannot function in these extreme orientations.

It was ultimately found that the sensor response was only marginally affected by the orientation of the sensor pair. This is illustrated in Fig. 6, which shows that rotation of the sensor away from zero results in a reduction of effective gain of up to 8% at 45º. Zero rotation is defined when two of the sides of the square field of view are parallel with the horizon. It does remain important that each differential pair is orientated correctly to prevent the controller behaving differently when rolled or pitched each way from the trim position.

3.0 AIRCRAFT MODELLING

For any dynamic model aircraft model to provide useful results, both the inertial characteristics and aerodynamic derivatives must be known or approximated. Given the apparent complexity of finding the moments of inertia by experiment (swinging the aircraft as a pendulum)[1,2], a solid CAD (CATIA) model was produced of the testbed aircraft (Fig. 7). It was envisaged that this approach would require less time, but also has two main advantages over the experimental option. First, CATIA will also calculate the products of inertia (one of which is used in the Aerosim inertial model) and secondly, this approach lends itself to modification of the airframe. The next intended variant would have the prop mounted higher allowing the inclusion of a rotating nose cone.

The aerodynamic derivatives can be measured experimentally through instrumented flights or wind tunnel testing. Alternatively, a basic estimation can be made from analysis of similar aircraft. In this case modified parameters for the Cessna C-172, supplied with the Aerosim toolset were used since the test aircraft is the same basic configuration and geometrically similar. This simplification was required to allow the project to be focused to more core activities such as sensor modelling. Any further work on this project should aim to better understand the aerodynamic performance and derivatives of the test aircraft.

Each sub-assembly was generated from measurements of the test aircraft; Density was applied to produce the correct component and total weights. The CG location, moments and product of Inertia I_{xx}, I_{yy}, I_{zz} and I_{xy} are then imported into a MAT-LAB configuration script which defines the aircraft parameters to be used for simulation.

4.0 AEROSIM – DYNAMIC AIRCRAFT MODEL

Figure 8 provides an overview of the Simulink model; the segments labelled 1-6 are as follows.

1. Aerosim 6-DOF Dynamic aircraft model
2. Aircraft state output, plotting and data logging
3. Atmospheric input parameters (ground-sky, max and min) and sensor self calibration
4. PID feedback controller – pitch and roll
5. Pitch and roll thermopile based sensors (analogue)
6. Digital processing and delay

The simulation is commenced with the aircraft in a userdefined state (attitude, roll and pitch rates, airspeed etc) and run at a fixed time step, typically 0·02sec (50hz). At each time step, the aircraft attitude is fed into to the atmosphere/thermopile model. The digital processing of the autopilot and resultant delays are simulated, with the output of the PID controller driving the servo motors, this completes the plant-control loop. The resultant aircraft motion is displayed during the simulation, and is also stored for later analysis.

Figure 9 shows a schematic of the Aerosim 6-DOF Dynamic aircraft model. This module is provided as part of the Aerosim package[7], it forms the heart of the dynamic simulation. All the relevant aircraft parameters are read from a MATLAB[6] *.mat file prior to the simulation run allowing for simple alteration of aircraft set-up or simulation of an entirely different aircraft utilising the same guidance system.

Figure 10 shows the calibration routine; simulating the pre-flight calibration of the aircraft, where the

minimum and maximum temperatures (sky and ground) are converted into ADC (analogue-to-digital converter) counts. Outputs display these values to the user and transfer these values to the digital processing in segment 6.

https://doi.org/10.1017/S0001924000000671 Published online by Cambridge University Press

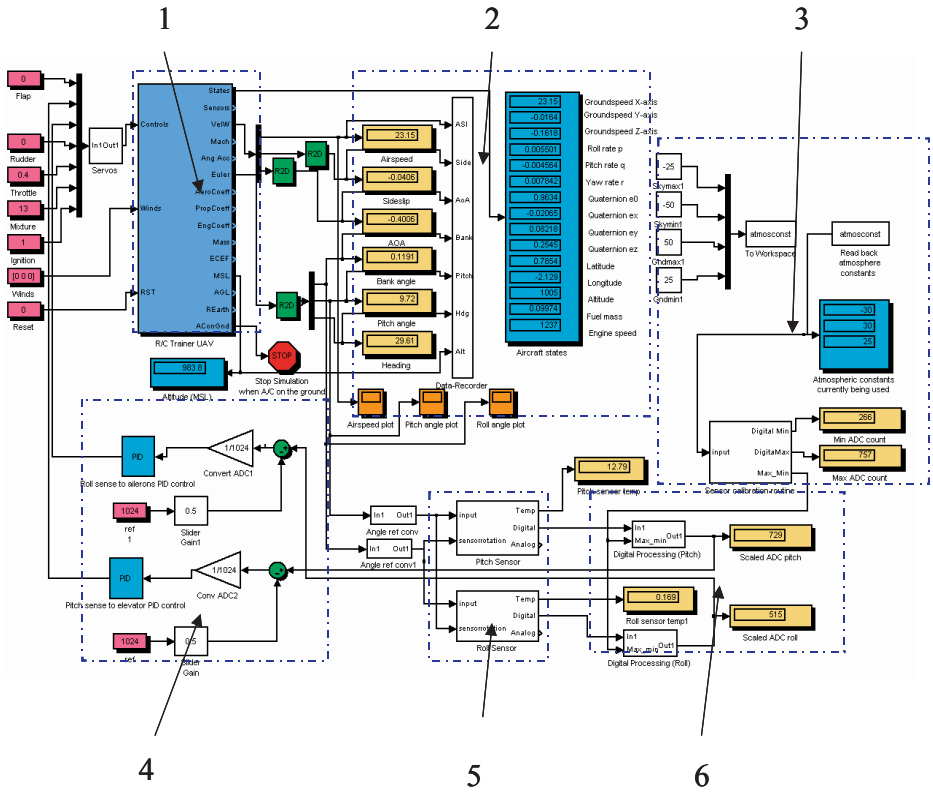


Figure 8. Simulink model incorporating sensor feedback control of the dynamic aircraft model.

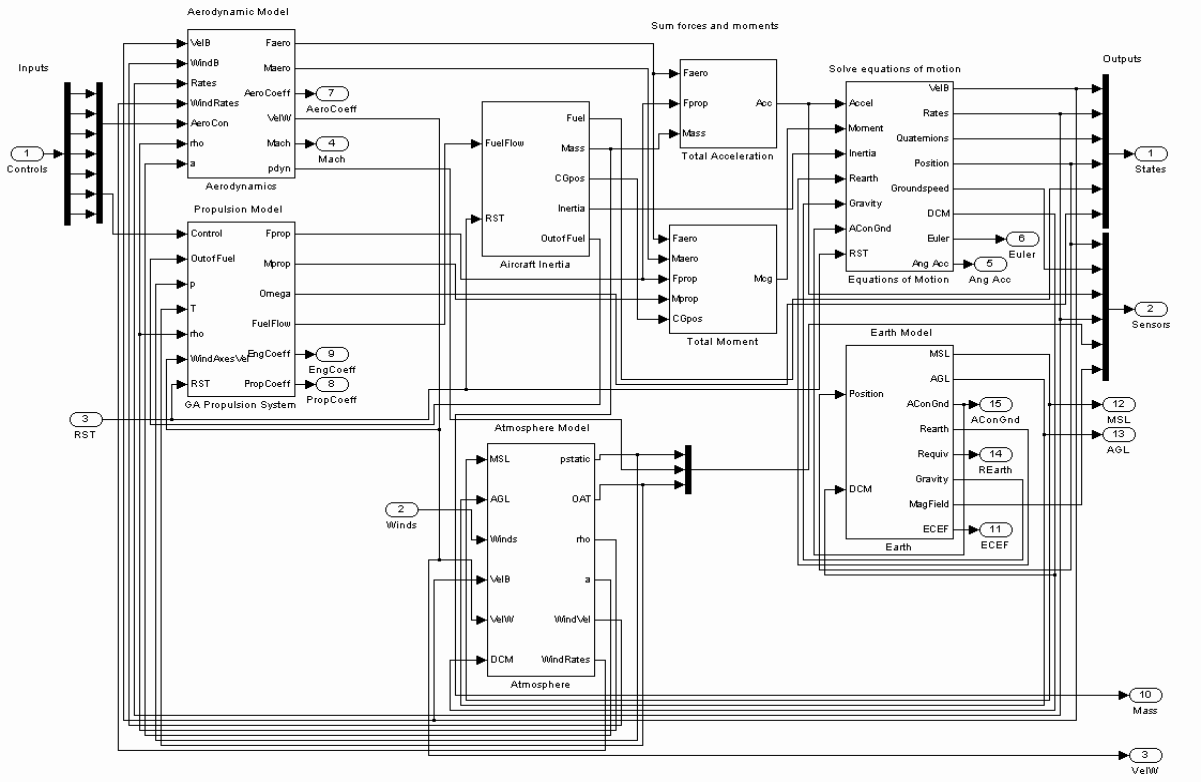


Figure 9. Inside the Aerosim 6–DOF aircraft model – Segment 1.

https://doi.org/10.1017/S0001924000000671 Published online by Cambridge University Press

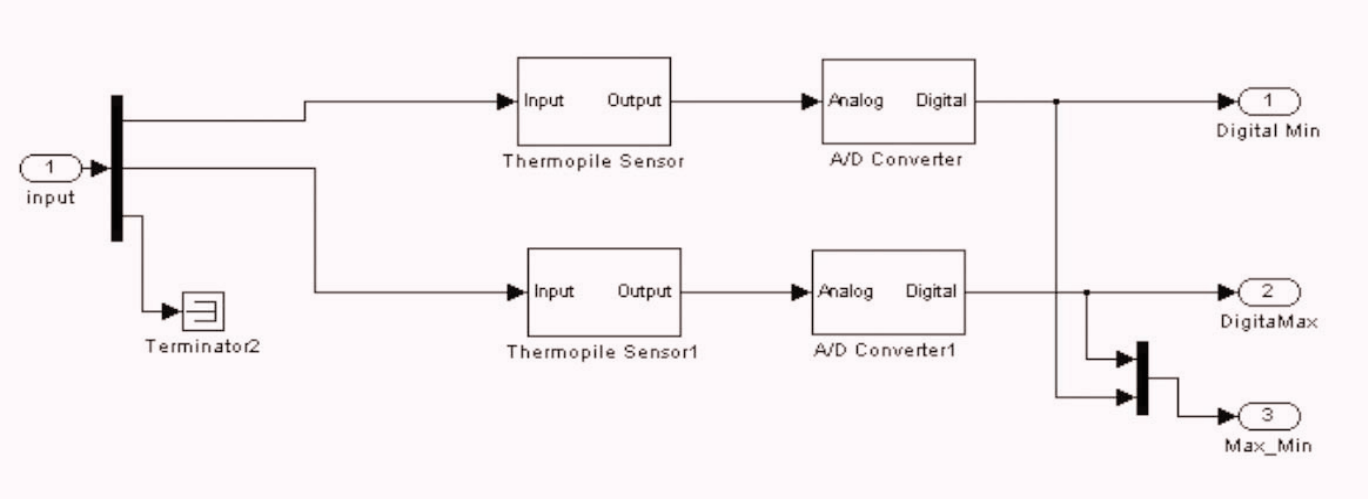


Figure 10. Thermopile sensor calibration to current atmospheric conditions – Segment 3.

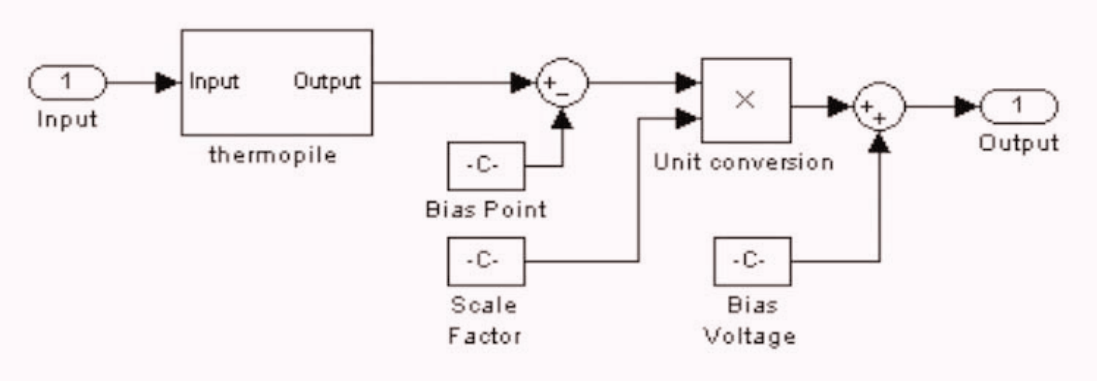


Figure 11. Thermopile analogue processing – zero offset and scale – Segment 5.

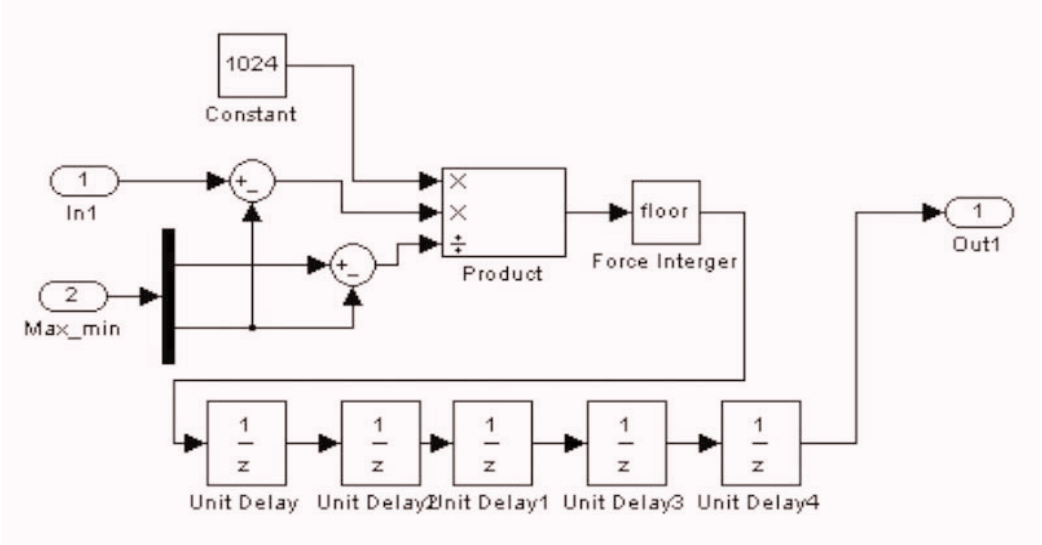


Figure 12. Digital processing and delay – Segment 6.

https://doi.org/10.1017/S0001924000000671 Published online by Cambridge University Press

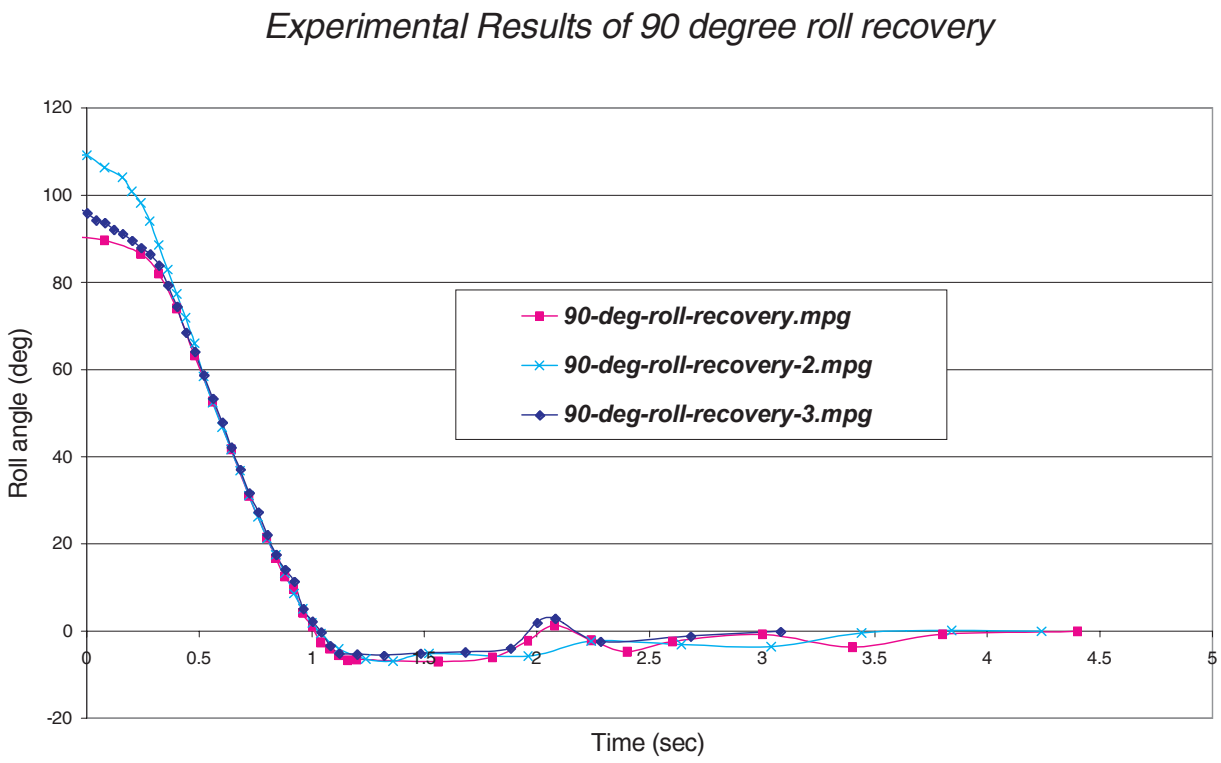


Figure 13. Flight test results of 90 degrees roll recovery.

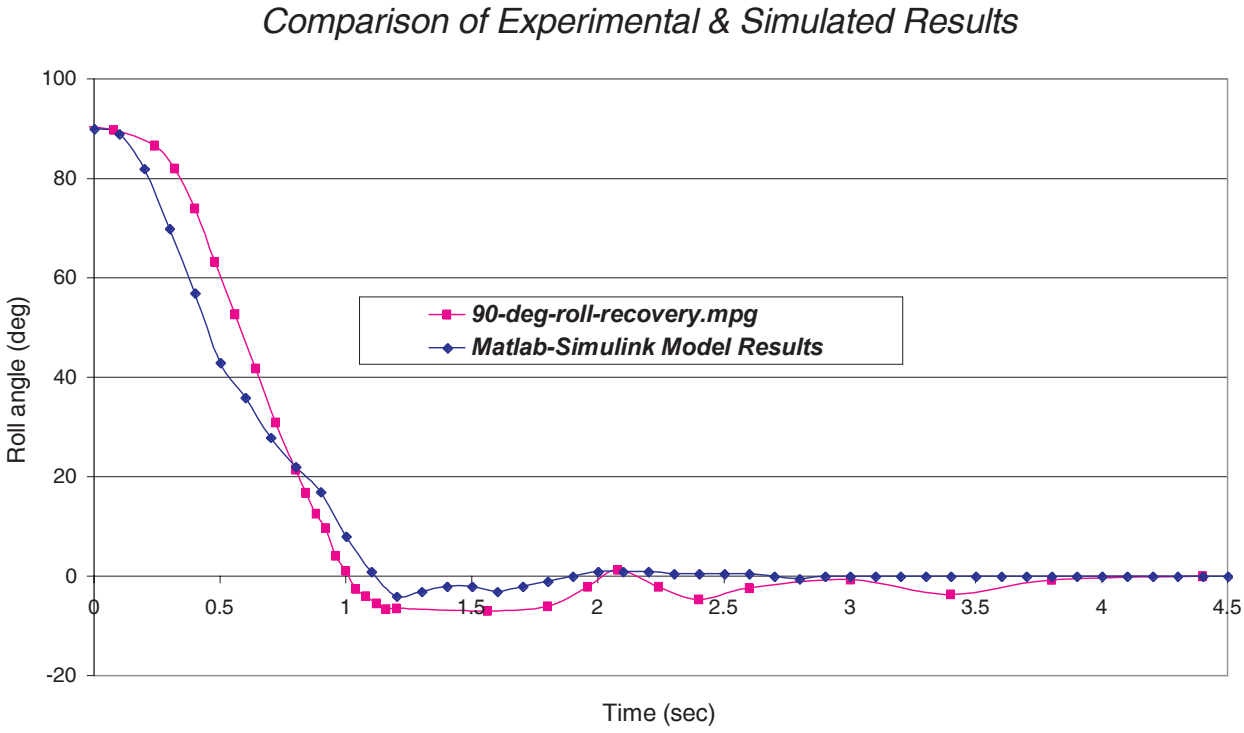


Figure 14. Experimental and simulated results show similar response rates and overshoot.

https://doi.org/10.1017/S0001924000000671 Published online by Cambridge University Press

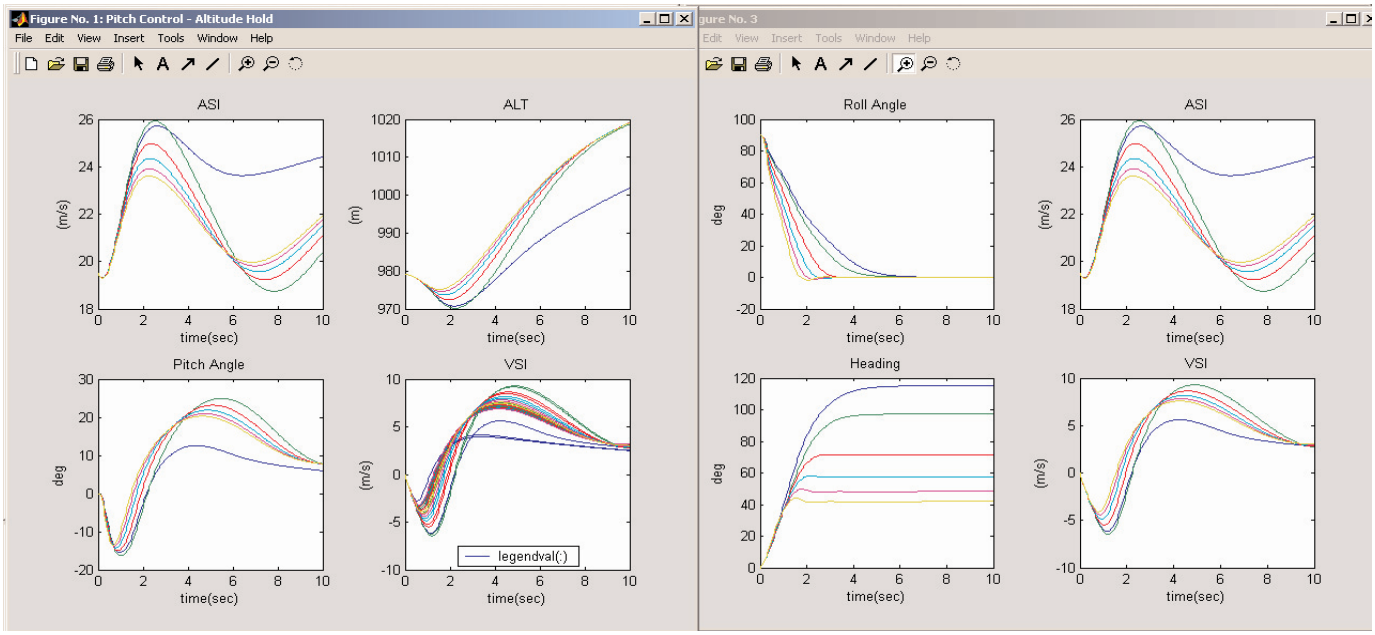


Figure 15. System response to varying control gains. 90 degree roll recovery with controller proportional gains from (10 to 60) × /180.

Note that the thermopile element in Fig. 11 is itself a two-dimensional lookup table for each axis, where the results are computed based on the aircraft orientation and atmospheric variables provided in segment 3 (see model overview – Fig. 8). This allows simulation of sensor rotation (φ) as described previously.

The digital processing segment shown in Fig. 12 is used to simulate the 8-bit micro-controller responsible for processing the sensor data and PID control loops. It essentially models the loss of precision through rounding and adds a delay representing the code execution time. The servo motor models from the Simulink[6] blockset allow input and output saturation limits, maximum rate and bandwidth of the actuators to be represented.

Given that the thermopile sensor bandwidth is approximately 30Hz, the servo motors and coupled control surfaces represent the major latency in the system, and thus the limitation for the maximum allowable controller gains for which the system is stable. The following parameters were used to model the servo actuators.

Max rate: 1·5rad/sec (86 deg/sec)

Bandwidth: 10Hz

5.0 RESULTS

As a test of the simulation's accuracy, the following manoeuvre was performed during flight testing. From steady state, straight and level flight, a manual snap roll is performed by the remote control pilot, at the instance of reaching 90º (such that the wings are now vertical) the autopilot is engaged and manual control ceases. The flight test was captured on digital video and later analysed using the VideoPoint frame capture software[9]. The aircraft response is plotted in Figs 13 and 14 from the instance of autopilot engagement. The three curves show the repeatability of the test procedure. Note that the pitch-roll interaction during this manoeuvre was minimal and was ignored principally because of the limitations of this test procedure. Any further flight-test validation would benefit greatly from the use of on-board instrumentation to accurately record the aircraft's dynamic response.

6.0 DISCUSSION

Actual flight-testing of the attitude stabilisation system has proven that the system does indeed function as intended. In some respects this work has been undertaken in reverse order, as the real system existed prior to this simulation project. Despite this, the simulation work provides two major outcomes. Firstly it verifies the process of operation based on independently sampled sensor data and shows similar behaviour to flight test results. Secondly, it can now serve as a tool to explore the limits of the autopilot functionality in terms of 'acceptable performance' for any given aircraft orientation and set of atmospheric conditions.

Based on the thermopile sensor data acquired, it appears that the autopilot performance would be degraded in situations of very low maximum temperature differential (MTD) between ground and sky. The errors created by non-uniform cloud cover or hot and cold patches on the ground are exacerbated in these situations. Despite this, the prototype system has flown successfully in hazy conditions where the MTD was only 3ºC. Safe operation inside dense cloud or those with significant vertical movement is not expected due to the MTD being very low, with the temperature profile possibly becoming inverted in these instances.

However, the systems performance in visual meteorological conditions (VMC) appears to be very good, even using only proportional control, as is currently the case on the test aircraft. The implementation of more sophisticated control algorithms may further improve the autopilot's performance. This work is currently underway along with a revision of the analogue electronics, providing higher resolution and thus better performance in low MTD conditions.

During the project a tool was developed to allow batch runs of the same model with varying controller gain settings. This allows verification of the performance of the system at a given setting but also allows a trial and error approach to tuning the PID control loop. Figure 15 shows a series of system responses to varying controller gains. This scenario is a 90º degree roll recovery run using controller proportional gains from (10 to 60) per degree.

https://doi.org/10.1017/S0001924000000671 Published online by Cambridge University Press

7.0 CONCLUSION

The functionality of the autopilot system based on thermopile sensors has been proven both theoretically and practically. The entire aircraft and autopilot system have been successfully modelled and verified utilising the Maple, Matlab and Simulink software tools[5,6]. The use of the 'Aerosim' Simulink block set [7] was instrumental to the project, providing the six degree of freedom aircraft model, to which all the additional systems could be grafted.

The model is now at the stage where it could be used to test system performance under different gain settings for the PID controller or even entirely new control strategies to see their impact on the resulting aircraft behaviour.

The current system appears suited to its intended market – low cost civilian UAVs where the mission often dictates operation in VMC conditions.

7.1 Suggested further work

The aerodynamic derivatives currently being used are based on an aircraft with the same basic geometric configuration. This is seen as a starting point only and further work with empirical methods, CFD or aerodynamic wind tunnel testing would likely provide better results, improving the accuracy of the simulation.

Fitting the test aircraft with inertial sensors or other attitude referencing systems would allow a much more detailed and complete comparison with the simulation. The current comparison is based on captured video footage of a single manoeuvre.

ACKNOWLEDGEMENTS

This project was conducted with support from the Undergraduate Research Opportunity Program (UROP) and the School of Aerospace, Mechanical and Manufacturing Engineering at RMIT University.

The authors wish to thank the Monash University UAV Group for their involvement and assistance throughout the practical flight test phase. In particular Ray Cooper for volunteering his excellent piloting skills during the test flights and to Brian Taylor[8] who is responsible for all of the actual UAV systems development, testing and construction.

REFERENCES

1. SOULE, H., MILLER, A. AND MARVEL, P. The experimental determination of the moments of inertia of airplanes, 1933, NACA Rep, No 467.
2. KIRSCHBAUM, H.W. Estimation of moments of inertia of airplanes from design data, 1936, NACA TN No 575.
3. SCHMIDT, W. and SCHIEFERDECKER, J. Understanding thermopile infrared sensors, Accessed 14 February 2003. http://optoelectronics.perkinelmer.com/library/papers/tp6.htm
4. Melexis datasheet for the MLX90247 thermopile sensor, Accessed 14 February 2003. http://www.melexis.com/prodmain.asp?search=thermopile&family=MLX90247
5. MAPLE, V. Release 4, Waterloo Maple, 1996.
6. Matlab/Simulink Version 6.0.0.88 Release 12, The MathWorks, ©1984-2000.
7. AeroSim aeronautical simulation blockset for Matlab, Unmanned Dynamics, Accessed 30 February 2003. http://www.u-dynamics.com/contact.htm
8. TAYLOR, B., BIL, C., WATKINS, S. and EGAN, G. Horizon sensing attitude stabilisation: A VMC Autopilot, 18th International UAV Systems Conference, 2003, Bristol, UK.
9. Videopoint Version 2.1, Lenox Softworks ©1999. http://www.lsw.com/videopoint

https://doi.org/10.1017/S0001924000000671 Published online by Cambridge University Press